

# The Pattern Speed of the Galactic Bar

Walter Dehnen

*Theoretical Physics, 1 Keble Road, Oxford OX1 3NP, United Kingdom; and  
Max-Planck Institut f. Astronomie, Königstuhl, D-69117 Heidelberg, Germany; dehnen@mpia-hd.mpg.de*

## ABSTRACT

Most late-type stars in the solar neighborhood have velocities similar to the local standard of rest (LSR), but there is a clearly separated secondary component corresponding to a slower rotation and a mean outward motion. Detailed simulations of the response of a stellar disk to a central bar show that such a bi-modality is expected from outer-Lindblad resonant scattering. When constraining the run of the rotation curve by the proper motion of Sgr A\* and the terminal gas velocities, the value observed for the rotation velocity separating the two components results in a value of  $(53 \pm 3) \text{ km s}^{-1} \text{ kpc}^{-1}$  for the pattern speed of the bar, only weakly dependent on the precise values for  $R_0$  and bar angle  $\phi$ .

*Subject headings:* Galaxy: kinematics and dynamics — Galaxy: structure — solar neighborhood

## 1. Introduction

Even though we now know beyond reasonable doubt that the Milky Way is barred, the structure of the bar, its orientation and pattern speed are still subject to substantial debate, mainly because of the edge-on view and dust obscuration. Consequently, the properties of the bar have been inferred rather indirectly from IR photometry (Blitz & Spergel 1991; Dwek et al. 1995; Binney et al. 1997), asymmetries in the distribution or magnitude of stars (Whitelock & Catchpole 1992; Weinberg 1992; Nikolaev & Weinberg 1997; Stanek 1995; Sevenster 1996; Stanek et al. 1997), and gas velocities (Liszt & Burton 1980; Binney et al. 1991; Englmaier & Gerhard 1999; Weiner & Sellwood 1999). While all these studies are based on observations of the inner Galaxy itself, it is the goal of this letter to constrain the properties of the bar by its effect on the stellar velocity distribution observed in the solar neighborhood.

## 2. The Local Stellar Velocity Distribution

In contrast to the structure of the inner Galaxy, the local stellar velocity distribution can be observed to much greater detail than for any external galaxy. Figure 1 shows the distribution  $f(u, v)$  in radial ( $u$ ) and rotational ( $v$ ) velocities (relative to the LSR) that has been inferred from the Hipparcos data (ESA 1997) of 6 018 late-type stars (Dehnen 1998 & 1999a).

This distribution shows a lot of structure, most of which is real (noise has been suppressed). Apart from an overall smooth background and a *low-velocity* region (solid ellipse in Fig. 1), within which  $f$  has several peaks associated with moving groups, there is also an *intermediate-velocity* structure (broken ellipse) containing  $\sim 15\%$  of the late-type stars but hardly any early-type stars, which mainly populate the moving groups (Dehnen 1998; Chereul et al. 1998; Asian et al. 1999; Skuljan et al. 1999). This secondary component, which consists predominantly of stars moving outwards ( $u < 0$ ) and is clearly separated from the low-velocity peak, was only vaguely recognizable in pre-Hipparcos data sets; the resulting mean outward motion of stars with  $v \lesssim -30 \text{ km s}^{-1}$  is also known as *u-anomaly*.

## 3. What Causes this Bi-Modality?

Attempts to explain this seeming anomaly by non-equilibrium dynamics, like the dispersion of a stellar cluster or the merger of a satellite, fail because of the exclusively late stellar type, disk-like kinematics ( $v$  nearly as LSR), and rather high metallicity (Raboud et al. 1998) of the intermediate-velocity stars. Thus, dynamical equilibrium must account both for the mean outward motion of

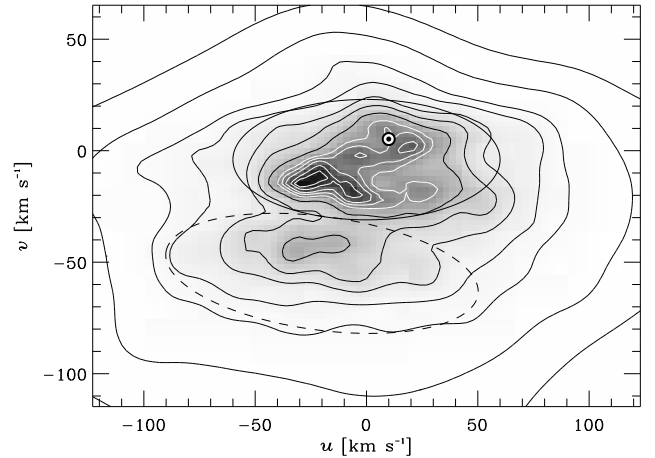


Fig. 1.— The distribution  $f(u, v)$  inferred from Hipparcos data for late-type stars (3 527 main-sequence stars with  $B-V \geq 0.6$  and 2 491 mainly late-type non-main-sequence stars, high-velocity stars excluded, see Dehnen 1998).  $u$  and  $v$  denote the velocities towards  $\ell = 0^\circ$  and  $\ell = 90^\circ$  w.r.t. the LSR measured by Dehnen & Binney (1998);  $\odot$  indicates the solar velocity. Samples of early-type stars contribute almost exclusively to the low-velocity region (solid ellipse). The region of intermediate velocities (broken ellipse) is mainly represented by late-type stars,  $\sim 15\%$  of which fall into this region.

the intermediate-velocity stars and for their clear separation from the low-velocity stars. The first fact rules out any axisymmetric equilibrium, while the second strongly hints towards an orbital resonance.

### 3.1. The Bar's Outer Lindblad Resonance

Such a resonance is provided by the Galactic bar: the outer Lindblad resonance (OLR), which occurs when

$$\Omega_b = \omega_\phi + \frac{1}{2}\omega_R. \quad (1)$$

Here,  $\omega_\phi$  and  $\omega_R$  are the azimuthal and radial orbital frequencies, while  $\Omega_b$  is the pattern speed of the bar. After each radial lobe, a star on a resonant orbit is at the same position w.r.t. bar, and hence, is always pushed in the same direction forcing it onto a different orbit. According to the modeling of the gas motions in the inner Galaxy (Englmaier & Gerhard 1999; Weiner & Sellwood 1999), the radius  $R_{\text{OLR}}$  corresponding to the OLR of circular orbits is not far from  $R_0$ .

Orbits inside (outside) the OLR, i.e. with  $\omega_\phi + \frac{1}{2}\omega_R > \Omega_b$  ( $< \Omega_b$ ), are elongated perpendicular (parallel) to the bar's major axis and are moving on average outwards (inwards) for bar angles  $\phi \in [0^\circ, 90^\circ]$ . The bar angle is defined as the azimuth of the Sun w.r.t. the bar's major axis and, according to IR photometry, lies in the range  $15^\circ$  to  $45^\circ$ .

Thus, the OLR of the Galactic bar can naturally explain the low- versus intermediate-velocity bi-modality of  $f(u, v)$ , provided the Sun is *outside* the OLR (Dehnen

1999a). In this picture, the depression between the modes of  $f(u, v)$  is due to exactly resonant orbits, and from the observed  $v$ -velocity of

$$v_{\text{OLR}} = (-31 \pm 3) \text{ km s}^{-1} \quad (2)$$

for the saddle point between the two modes, we can estimate that  $R_0 - R_{\text{OLR}} \simeq |v_{\text{OLR}}/v_0|R_0 \simeq 1 \text{ kpc}$  (for a flat rotation curve). Thus, only stars with epicycle amplitudes  $\gtrsim 1 \text{ kpc}$ , i.e. predominantly late-type stars, can visit us from inside the OLR, in agreement with the absence of early-type stars in the secondary component.

This proposal is in line with the ideas of Raboud et al. (1998), who observed a high metallicity and outward mean motion for disk stars with  $v < -30 \text{ km s}^{-1}$  and interpreted this as evidence for the Galactic bar, since in Fux's (1997)  $N$ -body simulations of the Milky Way  $\bar{u} < 0$  at the solar position. However, these authors did not relate the effect to the OLR nor were they able, for lack of resolution both in the data and the model, to make detailed quantitative investigations.

### 3.2. The Response of the Disk to a Stirring Bar

In order to quantify the behavior of a warm stellar disk in presence of a central bar, I performed numerical simulations in which a bar is grown in an initially axisymmetric exponential disk. These simulations, presented in detail in Dehnen (1999b), use a technique, which is similar to that of Vauterin & Dejonghe (1997) and allows for very high resolution.

The simulations show that a second mode appears in  $f(u, v)$  at many positions in the Galactic disk, provided the velocity dispersion is high enough. The velocity  $v_{\text{OLR}}$  of the division line between the modes depends essentially on four parameters: (1) our distance to the OLR, quantified by the ratio  $R_{\text{OLR}}/R_0$ ; (2) the bar angle  $\phi$ ; the (3) shape and (4) normalization of the rotation curve, quantified by  $\beta \equiv d \ln v_c / d \ln R$  and  $v_0 \equiv v_c(R_0)$ . The strength of the bar, its morphology, and the details of the stellar DF hardly affect the velocity  $v_{\text{OLR}}$ , but may change the strength of the secondary component.

The simulations used rotation curves  $v_c \propto R^\beta$  and a simple quadrupole to model the non-axisymmetric contribution of the bar potential. Figure 2 shows the resulting  $f(u, v)$  for  $\beta = 0$ ,  $\phi = 25^\circ$ , and three different values for  $\Omega_b$ , which is related to  $R_{\text{OLR}}$  by

$$\frac{R_{\text{OLR}}}{R_0} = \left( \frac{\Omega_0}{\Omega_b} \left[ 1 + \sqrt{\frac{1+\beta}{2}} \right] \right)^{1/(1-\beta)} \quad (3)$$

with  $\Omega_0 \equiv v_0/R_0$ . The secondary component is weaker and occurs at larger  $|v|$  the farther the OLR is from the

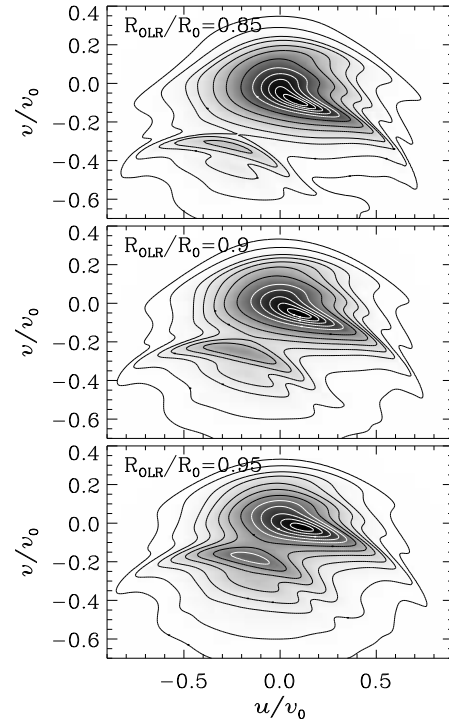


Fig. 2.— Simulated  $f(u, v)$  after the growth of a central bar. The initial axisymmetric disk has scale length  $0.33R_0$  and velocity dispersion reminiscent of the old stellar disk. The rotation curve is assumed flat and the bar angle is fixed at  $\phi = 25^\circ$ . The pattern speed decreases from top to bottom panel.

Sun. For  $15^\circ \leq \phi \leq 45^\circ$ ,  $-0.2 \leq \beta \leq 0.2$  and  $0.8 \leq R_{\text{OLR}}/R_0 \leq 0.95$ ,  $v_{\text{OLR}}$  is well approximated by

$$v_{\text{OLR}} \approx a \frac{1+\beta}{1-\beta} \left[ v_0 - \frac{R_0 \Omega_b}{1 + \sqrt{(1+\beta)/2}} \right] - (b + c\beta) v_0, \quad (4)$$

where the coefficients  $a$ ,  $b$ , and  $c$  are given in Table 1.

### 4. Implications for the Inner Galaxy

We now *assume* that the observed low- versus intermediate-velocity bi-modality of  $f(u, v)$  is caused by scattering off the OLR of the Galactic bar. Then the observed velocity  $v_{\text{OLR}}$  (2) constitutes a new constraint on the structure of

Table 1: Best-fit values for  $(a, b, c)$  in equation (4)

$\phi$	$a$	$b$	$c$
$15^\circ$	1.3549	0.0761	0.1362
$20^\circ$	1.2686	0.0642	0.1120
$25^\circ$	1.2003	0.0526	0.0892
$30^\circ$	1.1424	0.0406	0.0711
$35^\circ$	1.0895	0.0298	0.0538
$40^\circ$	1.0420	0.0200	0.0423
$45^\circ$	1.0012	0.0103	0.0316

Table 2: Adding the new constraint: fitting  $v_{\text{term}}$  for  $|\ell| > 30^\circ$ ,  $\mu_\ell$  of Sgr A\*, and  $v_{\text{OLR}}$ .

$R_0 = 7, v_0 = 198 \pm 5.6, \beta = -0.147 \pm 0.025$				$R_0 = 8, v_0 = 227 \pm 6.4, \beta = -0.020 \pm 0.022$			
$\phi$	$\Omega_b$	$R_{\text{OLR}}/R_0$	$R_{\text{CR}}/R_0$	$\phi$	$\Omega_b$	$R_{\text{OLR}}/R_0$	$R_{\text{CR}}/R_0$
15°	51.4 ± 1.4	0.920 ± 0.011	0.594	15°	50.5 ± 1.4	0.954 ± 0.010	0.567
20°	52.1 ± 1.5	0.909 ± 0.012	0.586	20°	51.1 ± 1.4	0.943 ± 0.010	0.561
25°	52.8 ± 1.5	0.898 ± 0.012	0.579	25°	51.8 ± 1.4	0.932 ± 0.010	0.554
30°	53.7 ± 1.5	0.886 ± 0.013	0.572	30°	52.5 ± 1.4	0.920 ± 0.010	0.547
35°	54.5 ± 1.6	0.874 ± 0.013	0.564	35°	53.2 ± 1.5	0.908 ± 0.011	0.540
40°	55.3 ± 1.6	0.863 ± 0.013	0.557	40°	53.8 ± 1.5	0.897 ± 0.011	0.533
45°	56.2 ± 1.6	0.851 ± 0.013	0.549	45°	54.5 ± 1.5	0.885 ± 0.011	0.526

$R_0 = 7.5, v_0 = 212 \pm 6, \beta = -0.080 \pm 0.024$				$R_0 = 8.5, v_0 = 241 \pm 6.8, \beta = 0.033 \pm 0.021$			
$\phi$	$\Omega_b$	$R_{\text{OLR}}/R_0$	$R_{\text{CR}}/R_0$	$\phi$	$\Omega_b$	$R_{\text{OLR}}/R_0$	$R_{\text{CR}}/R_0$
15°	50.8 ± 1.4	0.939 ± 0.010	0.581	15°	50.4 ± 1.4	0.967 ± 0.009	0.552
20°	51.5 ± 1.4	0.928 ± 0.011	0.575	20°	51.0 ± 1.4	0.956 ± 0.009	0.546
25°	52.2 ± 1.4	0.917 ± 0.011	0.568	25°	51.6 ± 1.4	0.944 ± 0.009	0.539
30°	52.9 ± 1.5	0.905 ± 0.011	0.560	30°	52.2 ± 1.4	0.932 ± 0.010	0.532
35°	53.7 ± 1.5	0.893 ± 0.012	0.553	35°	52.8 ± 1.4	0.921 ± 0.010	0.526
40°	54.4 ± 1.5	0.882 ± 0.012	0.546	40°	53.5 ± 1.5	0.909 ± 0.010	0.519
45°	55.2 ± 1.6	0.870 ± 0.012	0.539	45°	54.1 ± 1.5	0.898 ± 0.010	0.513

the inner Galaxy, the implications of which we will now investigate.

#### 4.1. Other Constraints

Unfortunately, the value of  $v_{\text{OLR}}$  does not depend on just one, but several parameters. Thus, in order to understand the implications of the observed value, we must combine the new constraint with other, independent constraints.

Determinations of the proper motion of Sgr A\*, the radio source associated with the Galactic center, yield (in  $\text{km s}^{-1} \text{kpc}^{-1}$ )  $\mu_\ell = -28.0 \pm 1.7$  (Reid et al. 1999) and  $\mu_\ell = -29.3 \pm 0.9$  (Backer & Sramek 1999), while the latitudinal proper motion  $\mu_b$  is negligible. Sgr A\* is generally thought to be associated with a black hole of mass  $\sim 2.6 \times 10^6 M_\odot$  (Eckart & Genzel 1997, Ghez et al. 1998), which because of energy equipartition must be (nearly) at rest w.r.t. its surroundings. Thus, the observed proper motion is entirely due to the reflex of our own rotation around the Galaxy, and we obtain

$$\Omega_0 = (29.0 \pm 0.8) \text{ km s}^{-1} \text{ kpc}^{-1} - v_\odot/R_0, \quad (5)$$

where  $v_\odot = (5.25 \pm 0.62) \text{ km s}^{-1}$  is the Sun's  $v$ -motion w.r.t. the LSR (Dehnen & Binney 1998).

In order to constrain the shape of the rotation curve, i.e. the parameter  $\beta$ , we use the terminal gas velocities inferred by Malhotra (1994, 1995) from various observations in HI and CO. For axisymmetric gas motions, the terminal velocity is related to the rotation curve by

$$|v_{\text{term}}| = v_c(R_0 |\sin \ell|) - v_c(R_0) |\sin \ell|, \quad (6)$$

while non-axisymmetric effects are likely to add small deviations to this relation.

#### 4.2. Adding the New Constraint

We now put the various constraints together by (i) assuming (reasonable) values for  $R_0$  and  $\phi$ , (ii) computing  $v_0 = \Omega_0 R_0$  using (5), (iii) fitting  $\beta$  to the observed terminal velocity curve, and (iv) deriving the bar's pattern speed  $\Omega_b$  from the constraint on  $v_{\text{OLR}}$  whereby using the approximation (4). Note that the bar angle becomes important only at stage (iv), i.e.  $v_0$  and  $\beta$  are already fixed once  $R_0$  is chosen.

For  $R_0 = 7, 7.5, 8,$  and  $8.5 \text{ kpc}$  and values of  $\phi$  in the range  $15^\circ$  to  $45^\circ$ , which is required for the bar's morphology to be both similar to that of external galaxies and consistent with IR photometry, Table 2 lists the results of this procedure when fitting  $v_{\text{term}}$  at  $|\ell| > 30^\circ$  (the results hardly depend to this limit).

An inspection of the table reveals that the derived value for  $\Omega_b$  is only weakly dependent on the assumed values for  $R_0$  and  $\phi$ :  $\Omega_b$  varies by about 10% with larger  $\phi$  corresponding to larger  $\Omega_b$ . Owing to this weak dependence, the pattern speed of the bar is rather tightly constrained even without accurate knowledge of  $(R_0, \phi)$ :

$$\Omega_b = (53 \pm 3) \text{ km s}^{-1} \text{ kpc}^{-1}. \quad (7)$$

Table 2 also lists estimates for  $R_{\text{OLR}}/R_0$  obtained from equation (3) and for  $R_{\text{CR}}/R_0$  obtained from the terminal velocities by the relation

$$(\Omega_b - \Omega_0)R_0 = \frac{v_{\text{term}}(\ell)}{\sin \ell} \Big|_{|\sin \ell|=R_{\text{CR}}/R_0}. \quad (8)$$

An error is not given, but the uncertainty is about 10%.

Amongst the three constraints used to derive  $\Omega_b$  the biggest uncertainty comes from the proper motion of Sgr A\* (and its interpretation as reflex of the solar motion). If in equation (5) one uses the value reported by Reid et al., instead of a weighted mean with Backer & Sramek's measurement, the resulting  $\Omega_b$  is about 2% smaller, while  $R_{CR}/R_0$  hardly changes.

The estimate (7) is also subject to systematic uncertainties, due mainly to the idealized model. Future simulations which allow for a more general Galactic rotation curve and bar potential and are fitted simultaneously to the gas motion of the entire inner Galaxy and the local stellar velocity distribution are likely to reduce these uncertainties considerably.

## 5. Conclusion

The simulations presented in Dehnen (1999b) and briefly reported in §3.2 show that the bar's OLR *inevitably* creates a bi-modality in  $f(u, v)$  over a wide range of positions in the Galactic disc. The low- versus intermediate-velocity bi-modality in  $f(u, v)$  observed for late-type stars (Fig. 1), has the same characteristics as these OLR features and is thus best identified as such.

This in turn allows the observed  $v$ -velocity separating the two modes to be used as a new constraint on the parameters of the inner Galaxy, notably the rotation curve, the bar's pattern speed and projection angle. In conjunction with constraints for the rotation curve from the terminal gas velocities and the proper motion of Sgr A\*, this results in a value for the bar's pattern speed of  $(53 \pm 3) \text{ km s}^{-1} \text{ kpc}^{-1}$ . The systematic uncertainty is likely similar in size to the internal error; both shall be reduced in more elaborate future modeling.

The values for the corotation radius implied by this pattern speed and the terminal gas velocities are between 0.5 and 0.6 times  $R_0$ , i.e. larger than the upper limit of 0.5 given by Englmaier & Gerhard (1999), but consistent with Weiner & Sellwood (1999). Given that IR photometry suggests a bar length  $R_b$  of about  $0.45R_0$ , this implies a ratio  $R_{CR}/R_b$  of about  $1.25 \pm 0.2$ , in agreement with the few estimates for external galaxies (Merrifield & Kuijken 1995; Lindblad et al. 1996; Gerssen et al. 1999) and simulations (Athanasoula 1992).

## References

- Athanasoula E., 1992, MNRAS, 259, 345  
 Asian R., Figueras F., Torra J., Chen B., 1999, A&A, 341, 427  
 Backer D.C., Sramek R.A., 1999, ApJ, 000, 000 (astro-ph/9906048)  
 Binney J.J., Gerhard O.E., Stark A.A., Bally J., Uchida K.I., 1991, MNRAS, 252, 210  
 Binney J.J., Gerhard O.E., Spergel D.N., 1997, MNRAS, 288, 365  
 Blitz L., Spergel D.N., 1991, ApJ, 379, 631  
 Chereul E., Cr ez e M., Bienaym e O., 1998, A&A, 340, 384  
 Dehnen W., 1998, AJ, 115, 2384  
 ———. 1999a, in Galaxy Dynamics, eds. Merritt, Valuri & Sellwood, ASP Conf. Ser., 182, 297 (astro-ph/9810320)  
 ———. 1999b, in preparation  
 Dehnen W., Binney J.J., 1998, MNRAS, 298, 387  
 Dwek E., Arendt R.G., Hauser M.G., Kelsall T., Lisse C.M., Mosely S.H., Silverberg R.F., Sodroski T.J., Weiland J.L., 1995, ApJ, 445, 716  
 Eckart A., Genzel R., 1997, MNRAS, 284, 576  
 Englmaier P., Gerhard O.E., 1999, MNRAS, 304, 512  
 ESA, 1997, The Hipparcos and Tycho Catalogues, ESA SP-1200  
 Fux R., 1997, A&A, 327, 983  
 Gerssen J., Kuijken K. & Merrifield M.R., 1999, MNRAS, 306, 926  
 Ghez A.M., Klein B.L., Morris M., Becklin E.E., 1998, ApJ, 509, 678  
 Lindblad P.A.B., Lindblad P.O. & Athanasoula E., 1996, A&A, 313, 65  
 Liszt H.S., Burton W.H., 1980, ApJ, 236, 779  
 Malhotra S., 1994, ApJ, 433, 687  
 ———. 1995, ApJ, 448, 138  
 Merrifield M.R., Kuijken K., 1995, MNRAS, 274, 933  
 Nikolaev S., Weinberg M.D., 1997, ApJ, 487, 885  
 Raboud D., Grenon M., Martinet L., Fux R., Udry S., 1998, A&A, 335, L61  
 Reid M.J., Readhead A.C.S., Vermeulen R.C., Treuhaft R.N., 1999, ApJ, 000, 000 (astro-ph/9905075)  
 Sevenster M.N., 1996, in Barred Galaxies, IAU Coll 157, eds. Buta R., Crocker D.A., Elmegreen B.G., ASP Conf. Ser., 91, 536  
 Skuljan J., Hearnshaw J.B., Cottrell P.L., 1999, MNRAS, 000, 000 (astro-ph/9905002)  
 Stanek K.Z., 1995, ApJ, 441, L29  
 Stanek K.Z., Udalski A., Szymanski M., Kaluzny J., Kubiak M., Mateo M., Krzeminski W., 1997, ApJ, 477, 163  
 Vauterin P., Dejonghe H., 1997, MNRAS, 286, 812  
 Weinberg M.D., 1992, ApJ, 384, 81  
 Weiner B.J., Sellwood J.A., 1999, ApJ, 000, 000 (astro-ph/9904130)  
 Whitelock P., Catchpole R., 1992, in The Center, Bulge, and Disk of the Milky Way, ed. Blitz L. (Dordrecht: Kluwer), 103